

Avatar Concept Slider: Controllable Editing of Concepts in 3D Human Avatars

Lin Geng Foo

Max Planck Institute for Informatics
Saarland Informatics Campus

lfoo@mpi-inf.mpg.de

Ajmal Saeed Mian

University of Western Australia
ajmal.mian@uwa.edu.au

Yixuan He

Singapore University of Technology and Design
yixuan_he@mymail.sutd.edu.sg

Hossein Rahmani Jun Liu

Lancaster University

{h.rahmani, j.liu81}@lancaster.ac.uk

Christian Theobalt

Max Planck Institute for Informatics
Saarland Informatics Campus

theobalt@mpi-inf.mpg.de

Abstract

Text-based editing of 3D human avatars to precisely match user requirements is challenging due to the inherent ambiguity and limited expressiveness of natural language. To overcome this, we propose the Avatar Concept Slider (ACS), a 3D avatar editing method that allows precise editing of semantic concepts in human avatars towards a specified intermediate point between two extremes of concepts, akin to moving a knob along a slider track. To achieve this, our ACS has three designs: Firstly, a Concept Sliding Loss based on linear discriminant analysis to pinpoint the concept-specific axes for precise editing. Secondly, an Attribute Preserving Loss based on principal component analysis for improved preservation of avatar identity during editing. We further propose a 3D Gaussian Splatting primitive selection mechanism based on concept-sensitivity, which updates only the primitives that are the most sensitive to our target concept, to improve efficiency. Results demonstrate that our ACS enables controllable 3D avatar editing, without compromising the avatar quality or its identifying attributes.

1. Introduction

Creating high-fidelity human avatars and editing them according to user demands has shown its importance in multiple scenarios such as game development, film production and virtual character creation for the metaverse and live streaming applications [1, 35, 37]. To meet this demand, many works [4, 12, 14, 15, 19, 21, 39] have made significant progress in generating 3D human avatars with simple yet

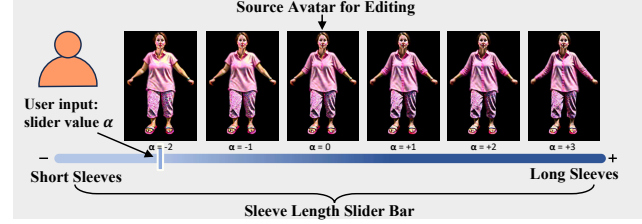


Figure 1. Illustration of our controllable concept editing. In this example, the user has provided text descriptions for two opposing ends of a concept: ‘short sleeves’ vs ‘long sleeves’. Our ACS allows users to specify the exact level of concept expression (e.g., sleeve length) that is desired, by moving the knob on the slider bar.

user-friendly language prompts, demonstrating a strong ability to generate high-fidelity and realistic avatars. At the same time, there has also been an increased demand for better control over the creation and customization of personalized digital avatars [40], e.g., changing the hair style, clothing, or adding some accessories to the avatar. To achieve this while avoiding the time-consuming process of repeated generation and prompt modifications, *avatar editing* techniques have emerged as a promising paradigm. These techniques aim to edit and sculpt some target details of an avatar while preserving most of the original identifying information.

Due to its importance, *avatar editing* has attracted much research attention recently [2, 9, 24, 40]. Drawing inspiration from the successes in harnessing diffusion models for 3D content generation [20, 28, 36], previous works such as Head-Sculpt [9] edit avatars by using an instruction-guided diffusion model [3]. Likewise, TECA [40] performs localized editing using a text-driven diffusion model with guidance

from a segmentation model [22]. Overall, these methods have led to advancements in text-based 3D avatar editing.

Despite the significant progress, existing 3D avatar editing methods [9, 40] are limited due to their reliance on text prompts as the sole guidance signals. Specifically, text prompts can be quite ambiguous, making it difficult to edit the avatar to *precisely align with* the users’ expectations. For instance, to describe the desired hair length of a human avatar, users may prefer descriptive words such as ‘long’ or ‘short’ – which are ambiguous and limited in expressing the exact degree of length. Moreover, this difficulty in achieving precise editing with text alone becomes even more evident when manipulating complex concepts like ‘sharpness’ of facial features, or other adjectives which may be hard to put into words, e.g., ‘kind’ or ‘evil’.

Driven by the problems mentioned above, our aim is to *precisely edit target concepts* of avatars in a convenient manner, akin to moving the knob on a continuous slider bar, from which users may select *exact values along the bar* to specify their desired avatar. An overview is shown in Fig. 1. However, achieving this aim is challenging, because: ① For each concept (e.g., body shape), it can be challenging to find such a continuous bar to express the intermediate degree of avatar concepts, since these concepts are often high-level abstract concepts that exist beyond the pixel level. This makes it difficult to identify where these high-level concepts reside in feature space, as well as pinpoint the precise axes that link the two opposing ends of a specific concept within the large feature space. ② Furthermore, it is challenging to isolate and edit only the desired concept without changing other identifying information of the avatar. This is because each avatar is generated with a mixture of elements, such as face shape, hairstyle, and clothing type, which are also entangled with concepts such as gender, race, and age. While editing the target concept, we may inevitably alter other attributes that we want to retain, and it is challenging to prevent this from happening.

In this work, we propose a novel Avatar Concept Slider (ACS) for 3D human avatar editing, which enables users to edit their 3D avatar precisely towards the desired degree of expression of a given concept, offering much more controllable editing of concepts than with text inputs alone. To overcome the three challenges highlighted above, our ACS comprises three corresponding designs, as follows: ① To pinpoint the precise concept axes that link the two opposing ends of a specific concept, we introduce the Concept Sliding Loss based on Linear Discriminant Analysis (LDA) to fine-tune an adapter. This facilitates precise slider-like editing using the score distillation sampling (SDS) optimization editing pipeline. LDA facilitates the identification of continuous axes (which we call the concept axes) that are the most discriminative in linking the two opposing sides of the user-provided concept. ② To preserve key identifying

attributes during editing, we further devise an Attribute Preserving Loss based on Principal Component Analysis (PCA), leveraging PCA to extract key attribute information from the features that are orthogonal to the target concept. Then, by encouraging these key attribute information to be retained, it enables users to edit their target concept in isolation, disentangled from other identifying attributes. ③ Moreover, we further propose a 3DGS primitive selection mechanism based on their concept-sensitivity, which enables us to selectively optimize a small set of the most crucial Gaussian primitives to reduce redundancy and improve efficiency.

With the above designs incorporated into the deployed ACS, users can input descriptions of two opposing ends of a target concept, e.g., with a pair of text phrases. Subsequently, users can precisely adjust the degree of expression of a desired concept on a given avatar, by simply moving a knob across a slider bar, achieving controllable editing.

2. Related Work

Text-Driven 3D Human Avatar Generation. To streamline the labour-intensive 3D avatar creation process, many recent works [4, 12, 14, 15, 19, 39, 41] focus on text-driven 3D avatar generation, relying solely on text prompt inputs to create a desired high-fidelity 3D human avatar. One line of works optimize their avatar model with text guidance in CLIP [29] space, e.g., AvatarCLIP [12]. Subsequent works such as DreamHuman [19], DreamAvatar [4], DreamWaltz [14], AvatarVerse [39], and TEDRA [32] rely on a text-to-image 2D diffusion prior (e.g., [30, 42]) to optimize their 3D avatar via an SDS optimization pipeline [28]. Recently, HumanGaussian [21] proposes to use 3DGS to represent the human avatar, resulting in faster convergence and high-quality avatars. However, these text-driven avatar generation methods are limited by the expressivity and ambiguity that is inherent in language, and often struggle with precisely generating the user-desired avatars with text prompts alone.

Text-Driven 3D Human Avatar Editing. Besides generation, some works [2, 24, 40] focus on editing existing 3D human avatars, sculpting the avatars according to the desired shape and texture. AvatarStudio [24] presents a text-driven method to edit head avatars based on the neural volumetric scene representation [34]. TECA [40] leverages a segmentation model to achieve localized editing based on text prompts. Another related line of works [5, 10, 45] further investigates the editing of entire 3D scenes via text instructions. Despite impressive generation and editing results, these methods are limited by their reliance on language instructions, which can be ambiguous regarding the degree of expression of the target concept. Orthogonal to these works, our paper aims at improving the controllability of 3D avatar editing methods, enabling users to edit the avatar more precisely towards the desired degree of a target concept.

Controllable Editing. Controllable editing methods are

increasingly crucial for enhancing generative flexibility in real-world applications. In the image domain, ControlNet [43] is a representative work which enables the conditioning of image generation on different controls, beyond text-based inputs. Subsequent works [7, 16, 44] explore this further, controlling the spatial layouts [44], injecting different conditions [16], or editing specific concepts in images [7]. Differently, we are the first to explore controllable 3D human avatar editing, by precisely controlling their concepts via a slider. Our proposed ACS enables precise control via a slider, which is integrated into the SDS distillation pipeline and adjusts the concepts distilled into the 3D avatar. To achieve controllability and identity preservation, we also introduce an LDA-based Concept Sliding Loss and PCA-based Attribute Preserving Loss.

3. Background: SDS Optimization Pipeline

Score Distillation Sampling (SDS) [28] leverages 2D diffusion models as a strong prior for 3D representation learning, e.g., text-to-3D content generation [15, 20] and 3D avatar editing [24]. Given a 3D representation θ (e.g., NeRF [25], 3DGS [18]), SDS optimization pushes the renderings of the 3D representation towards the target distribution (e.g., high-quality natural images), by distilling the predicted score from a pre-trained 2D diffusion prior. Thus, by using text-to-image diffusion models [30], we can facilitate text-to-3D generation by optimizing the 3D representation via SDS.

Specifically, we consider the case where a latent diffusion model (e.g., Stable Diffusion [30]) is used, which is denoted as $\epsilon_\phi(\cdot)$. SDS optimization starts by rendering the initial 3D representation θ into 2D images, and encoding them into latent space to obtain the initial latent features as \mathbf{z}_0 . Then, to derive the SDS loss \mathcal{L}_{SDS} , noise is added to the latent features \mathbf{z}_0 based on t steps of forward diffusion [30] to obtain the noised latents \mathbf{z}_t , where the SDS loss aims to denoise \mathbf{z}_t . Therefore, the gradient of the SDS loss with respect to the 3D representation θ can be formulated as: $\nabla_\theta \mathcal{L}_{SDS}(\phi, \mathbf{z}_0) = \mathbb{E}_{t, \epsilon} [w(t)(\epsilon_\phi(\mathbf{z}_t; y, t) - \epsilon) \frac{\partial \mathbf{z}_0}{\partial \theta}]$, where $w(t)$ is a weighting function that depends on time step t , and y is a text prompt that describes the desired 3D output.

Notably, to add functionalities, control options, or editing capabilities (e.g., with dense pose [39], face landmarks [4]) to the SDS optimization process while leveraging a pre-trained diffusion model, many works use LoRA adapters [13]. Specifically, for a selected set of weight parameters (denoted as ϕ_0) in the diffusion prior ϵ_ϕ , LoRA aims to learn a low-rank weight shift $\Delta\phi$ to obtain adapted weights $\hat{\phi}$ as: $\hat{\phi} = \phi_0 + \alpha\Delta\phi$, where α is the *scale factor* of the weight shift. By adapting the diffusion prior ϵ_ϕ with $\Delta\phi$ and α , the SDS optimization can be defined as:

$$\nabla_\theta \mathcal{L}_{SDS}(\phi, \mathbf{z}_0) = \mathbb{E}_{t, \epsilon} \left[w(t) \left(\epsilon_\phi(\mathbf{z}_t; y, t, (\Delta\phi, \alpha)) - \epsilon \right) \frac{\partial \mathbf{z}_0}{\partial \theta} \right]. \quad (1)$$

Overall, this mechanism allows us to efficiently adapt a diffusion model with a small set of parameters $\Delta\phi$ to cater for specific requirements, e.g., for editing, or for using additional control information. Hence, we also adopt the SDS optimization and LoRA adapter pipeline in Eq. 1.

4. Method: Avatar Concept Slider

To customize a human avatar, previous text-driven 3D avatar editing methods [9, 24, 40] are limited in terms of precision of concepts. To overcome this limitation, this paper aims to achieve controllable manipulation of 3D avatars towards a target concept in a convenient manner, akin to sliding a knob along a slider bar. However, achieving this goal is challenging due to the reasons outlined in the introduction. To address these challenges, we propose our Avatar Concept Slider (ACS), discussed in the following subsections. In Sec. 4.1, we address challenge ① by leveraging LDA and devising a sliding loss to enable slider-like precise control of the editing process. To tackle challenge ②, discussed in Sec. 4.2, we augment the sliding loss with an attribute-preserving loss based on PCA, ensuring concept-specific editing that is disentangled from the identifying attributes to be preserved. Lastly, in Sec. 4.3, we introduce a concept-sensitivity-based primitive selection mechanism, facilitating faster editing via selective optimization of our avatar’s 3DGS primitives. Overall, our pipeline is built upon SDS optimization (introduced in Sec. 3), and our full method is illustrated in Fig. 2.

4.1. Precise Slider-like Concept Editing

To precisely control the 3D avatar editing towards a specific degree of the target concept, the first challenge is to identify the continuous and discriminative axes connecting two opposing extremes of the concept. This can be challenging because the concepts are often abstract and high-level, making it difficult to pinpoint where exactly these opposing sides and their connecting axes reside in the large feature space. To overcome this, we leverage LDA to identify the continuous concept axes between the user-provided pair of descriptions for the two opposing sides, by directly computing the axes that are the most discriminative to link the opposing sides within the large feature space. Then, based on the identified concept axes, we introduce a Concept Sliding Loss (\mathcal{L}_{CS}) to fine-tune an adapter, which enables controllable and precise concept-specific editing via SDS optimization (Sec. 3). Below, we first describe how we identify the concept axes, before discussing the Concept Sliding Loss.

Concept Axes Identification with LDA. First, we aim to identify the continuous concept axes between the user-provided descriptions that represent two opposing sides of

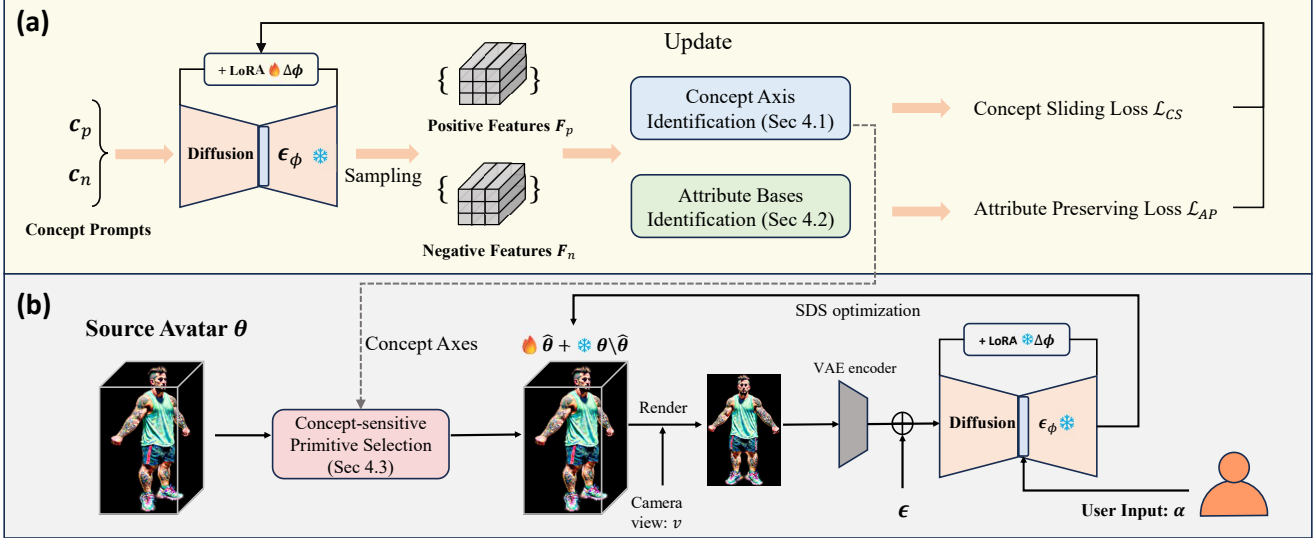


Figure 2. (a) Overview of the fine-tuning stage, where an adapter is fine-tuned to learn slider-like capabilities. Firstly, using the provided descriptions of the positive (c_p) and negative (c_n) side of the concept, we extract the corresponding positive and negative features. Then, to fine-tune the adapter $\Delta\phi$, our proposed Concept Sliding Loss (Sec. 4.1) is applied to learn the ability to slide across opposing ends of the target concept. The attribute-preserving loss (Sec. 4.2) helps to retain the key identifying attributes of the avatar. (b) After fine-tuning, the adapter is applied in an SDS optimization pipeline to achieve controllable concept-specific 3D avatar editing. The proposed 3DGS primitive selection mechanism (Sec. 4.3) further improves efficiency, by optimizing only the most related primitives to the target concept.

the target concept, where each point on the axis represents an intermediate degree of expression of the concept. By identifying the concept axes, we can *precisely control the transitioning of the concept* from one end to the other, and facilitate the learning of sliding capability via the sliding loss, enabling users to select any intermediate point along the concept axes for precise editing. Yet, this task is not straightforward. For instance, a simple solution may be to interpolate the semantic embeddings of two concept extremes, but such simple interpolation operations in a high-dimensional space often incurs high information redundancy and concept entanglement, incorporating many other unrelated concepts.

Therefore, to handle this challenge, we leverage LDA. LDA [11, 23] is a statistical technique that aims to identify the most discriminative axes that well-separate different groups/classes of data samples, even while using a low dimensional representation. Thus, by employing LDA, we can directly compute a set of low-rank axes that are the most discriminative and crucial to link the opposing concepts (and their corresponding sets of features) within the large feature space. Specifically, we harness LDA to exploit the latent space of the pre-trained text-to-image diffusion model used during SDS optimization (Sec. 3) to facilitate understanding of the target concept in a high-quality latent space.

Here, we first present the details of how we identify the concept axes. For simplicity, we explain it in the context of two-class LDA – where only positive and negative prompts are provided, although we can potentially use more classes (explained at the end of Sec. 4.1). In this

case, at the beginning, the user provides a pair of text prompts representing the positive (c_p) and negative (c_n) sides of a concept. Then, based on these prompts, we sample two sets of latent features from the diffusion model ϵ_ϕ by running the generation process N_s times for each of the positive and negative sides, where we perform sampling over different diffusion timesteps using different seeds. This yields two sets of features $\{\mathbf{F}_{p,i,x}\}_{i \in [1, N_s], x \in [1, C]}$ and $\{\mathbf{F}_{n,i,x}\}_{i \in [1, N_s], x \in [1, C]}$ corresponding to the positive and negative sides, where C refers to the channel dimensions of latent features. Each feature vector is D -dimensional, i.e., $\mathbf{F}_{p,i,x} \in \mathbb{R}^D$, $\mathbf{F}_{n,i,x} \in \mathbb{R}^D$.

We then start the LDA analysis [11, 23] using these two feature sets for the two opposing sides of the target concept. Specifically, we first compute both the within-class scatter ($\mathbf{S}_w \in \mathbb{R}^{D \times D}$) and the between-class scatter ($\mathbf{S}_b \in \mathbb{R}^{D \times D}$), where \mathbf{S}_w quantifies how much individual feature vectors deviate from their corresponding set centroids, while \mathbf{S}_b measures the deviation between the centroids of both sides of the concept (more details in Supplementary). Then, using \mathbf{S}_b and \mathbf{S}_w , the goal of LDA is to find *concept axis* $\mathbf{b}_c \in \mathbb{R}^D$, such that the projection of each feature vector onto the concept axis \mathbf{b}_c leads to maximal ratio of \mathbf{S}_b to \mathbf{S}_w . Intuitively, this encourages the feature vectors from both sets to be separated and positioned far from each other along the concept axis, while the feature vectors from the same set become tightly clustered along the concept axis. By doing so, LDA effectively pinpoints the direction of a concept axis, along which the opposing ends of the concept reside.

Specifically, this process can be expressed as the following optimization problem:

$$\mathbf{b}_c = \arg \max_{\mathbf{w}} \frac{\mathbf{w} \mathbf{S}_b \mathbf{w}^T}{\mathbf{w} \mathbf{S}_w \mathbf{w}^T}, \text{ s.t. } \|\mathbf{w}\| = 1, \quad (2)$$

where the numerator ($\mathbf{w} \mathbf{S}_b \mathbf{w}^T$) and denominator ($\mathbf{w} \mathbf{S}_w \mathbf{w}^T$) on the right hand side of Eq. 2 represent the projected scatters over the concept axis, and we want to find a concept axis \mathbf{b}_c that maximises their ratio while constraining \mathbf{w} to be a unit vector. Notably, the solution to Eq. 2 can be conveniently computed as the leading eigenvector of $\mathbf{S}_w^{-1} \mathbf{S}_b$ (refer to Supp). We highlight that these concept axes \mathbf{b}_c which are found by LDA are the most discriminative low-rank axes which best separates the positive and negative classes.

In practice, we can use more than 2 classes/groups of features. For instance, we can include three classes: positive, neutral, and negative, allowing us to compute two concept axes via LDA that hold strong discriminative power between these classes in the latent space, which are orthogonal to each other. We can then apply our sliding loss onto both concept axes for a stronger effect. Note that, even more classes can be included (with more prompts), but we found that using 3 classes is usually sufficient to obtain good results in practice.

Concept Sliding Loss. The above process identifies the concept axes which represents the continuous transition between the two opposing sides of the target concept. Based on the identified concept axes, we introduce a Concept Sliding Loss to fine-tune an adapter to facilitate concept-specific editing of the 3D avatar. Since we adopt the SDS optimization pipeline (Sec. 3) to edit the 3D avatar via a pre-trained diffusion model, we aim to incorporate such concept-specific slider-like editing abilities into it. Hence, we propose a Concept Sliding Loss (\mathcal{L}_{CS}) to impart such concept transitioning abilities to the adapter, enabling us to precisely control the editing through a scale factor α in Eq. 1.

Intuitively, our Concept Sliding Loss \mathcal{L}_{CS} facilitates the controlled movements of features along the concept axis towards a specified intermediate point, which is specified by the user as a *slider interpolation factor*. Specifically, to control such movements of features during editing, our loss fine-tunes the adapter ($\Delta\phi$) such that the scale factor α in Eq. 1 gains the ability as the *slider interpolation factor*. Thus, at deployment, with the user-provided interpolation factor $\hat{\alpha}$, we can set it as the scale factor (i.e., setting $\alpha = \hat{\alpha}$), thus allowing the adapted diffusion model to precisely locate the desired intermediate point on the concept axes. The Concept Sliding Loss \mathcal{L}_{CS} , when using only positive and negative concept prompts, is defined as:

$$\begin{aligned} \mathcal{L}_{CS}(\Delta\phi) = & \mathbb{E}_{\alpha_1, \alpha_2} \left[\left\| \left(\text{Proj}(\mathbf{f}(\alpha_1, \Delta\phi, c_{nu}), \mathbf{b}_c) - \text{Proj}(\mathbf{f}(\alpha_2, \Delta\phi, c_{nu}), \mathbf{b}_c) \right) \right. \right. \\ & \left. \left. - \left(\text{Proj} \left(\frac{1 + \alpha_1}{2} \mu_p + \frac{1 - \alpha_1}{2} \mu_n, \mathbf{b}_c \right) - \text{Proj} \left(\frac{1 + \alpha_2}{2} \mu_p + \frac{1 - \alpha_2}{2} \mu_n, \mathbf{b}_c \right) \right) \right\|^2 \right], \end{aligned} \quad (3)$$

where $\mathbf{f}(\cdot)$ represents the generation of latent features, c_{nu} is a neutral text prompt template, $\mu_p, \mu_n \in \mathbb{R}^D$ are computed mean vectors for the positive and negative con-

cept sides (see Supp for more details), and we select various points α_1, α_2 in the range $[-1, 1]$ to represent intermediate concepts; $\text{Proj}(\cdot, \mathbf{b}_c)$ is the projection operator, which projects the features onto the concept axes \mathbf{b}_c , where $\text{Proj}(x, \mathbf{b}_c) = \frac{x \cdot \mathbf{b}_c}{\mathbf{b}_c \cdot \mathbf{b}_c} \mathbf{b}_c^T$. Intuitively, this loss encourages the latent feature's movements along the concept axes (after applying the slider scale factor) to match the reference movements as calculated with the aid of the positive and negative concept text prompts. The latter is computed using the interpolations between μ_p and μ_n as: $(\frac{1+\alpha_1}{2} \mu_p + \frac{1-\alpha_1}{2} \mu_n)$ and $(\frac{1+\alpha_2}{2} \mu_p + \frac{1-\alpha_2}{2} \mu_n)$. Moreover, our loss is applied to encourage precise movements of the slider, and do not penalize the actual locations of latent features on the concept axes. This minimizes “calibration” issues during training where the source avatar is not neutral, e.g., when an “old man” is given the source avatar, we do not assume that the source avatar is at scale factor of “0”.

Overall, this loss can fine-tune the adapter parameters $\Delta\phi$ such that the SDS optimization pipeline in Eq. 1 can be used to smoothly edit our avatar by adjusting the scale factor α during editing. Note that this loss can also be expanded to include more than two classes, where the dimensions of \mathbf{b}_c are expanded, and concept means are also adapted to include the new features (e.g., neutral features). Also note that, with this loss design, we only need to identify the concept axes once (via LDA), and it can be used for the entire adapter fine-tuning process. Please refer to Supp for more details.

4.2. Preserving of Identity-related Attributes

While the Concept Sliding Loss presented above facilitates learning and representing intermediate points between opposing sides of a concept, it may inadvertently alter other identifying attributes of the avatar that we want to retain. This challenge arises as the 3D avatars contain many elements (e.g., face shape, hairstyle and clothing type) that involve entangled concepts such as gender, race, and age, as highlighted in challenge ② in the introduction. Thus, it can be challenging to retain these other identifying information of the avatar while editing the desired concept.

To address this, we leverage Principal Component Analysis (PCA) to disentangle the concepts of the avatar and retain key identifying attributes. PCA helps to identify a small set of highly informative bases that are orthogonal to our concept axes, *representing key identifying attributes unrelated to the target concept*, but which can explain the other key variations in the latents. Based on these key attribute bases found via PCA, we propose an Attribute Preserving Loss \mathcal{L}_{AP} , enabling fine-tuning of the adapter to preserve identifying attributes. Below, we first discuss the bases identification with PCA, followed by the attribute preserving loss.

Attribute Bases Identification with PCA. Firstly, we reuse the features ($\mathbf{F}_{p,i,x}$ and $\mathbf{F}_{n,i,x}$) that were computed in Sec. 4.1, which represent the positive and negative sides

of the target concept. Then, we run PCA analysis on these features to identify a small set of key attributes in the feature space that are not related to our target concept. This is achieved through finding the K principal components (i.e., orthogonal bases $\{\mathbf{b}_{a,k}\}_{k=1}^K$) which are orthogonal to our concept axes. Specifically, one way of performing PCA is through iteratively searching for the next principal component, which explains as much of the remaining variance of the data as possible, while being orthogonal to the previous identified principal components. Here, we recurrently employ this PCA technique to compute the main component bases orthogonal to our concept axis \mathbf{b}_c , formulated as:

$$\mathbf{b}_{a,k} = \arg \max_{\mathbf{w}} \frac{\mathbf{w} \hat{\mathbf{F}}_k \hat{\mathbf{F}}_k^T \mathbf{w}^T}{\mathbf{w} \mathbf{w}^T}, \text{ where } \hat{\mathbf{F}}_k = \hat{\mathbf{F}} - \sum_{j=1}^{k-1} \hat{\mathbf{F}} \mathbf{b}_{a,j-1}^T \mathbf{b}_{a,j-1}, \quad (4)$$

where $\hat{\mathbf{F}} \in \mathbb{R}^{D \times (2 \cdot N_s \cdot C)}$ is the combined merger of both positive and negative sets of features ($\{\mathbf{F}_{p,i,x}\}_{i \in [1, N_s], x \in [1, C]}$ and $\{\mathbf{F}_{n,i,x}\}_{i \in [1, N_s], x \in [1, C]}$), and \mathbf{w} is constrained to be a unit vector. Crucially, by treating the first ‘principal component’ $\mathbf{b}_{a,0}$ as our concept axes \mathbf{b}_c identified in Eq. 2 and iteratively solving Eq. 4 for $k = \{1, \dots, K\}$, we can obtain K key attribute bases $\{\mathbf{b}_{a,k}\}_{k=1}^K$ that best explain the remaining variance in the features. Furthermore, these obtained bases are orthogonal to our concept axis \mathbf{b}_c which are the key discriminative concept axes, which suggests that these bases are unrelated to the target concept. Note that, although the small set of K attribute bases has only a low rank, they capture the most important identifying information in the avatar (that are unrelated to the target concept), which should be retained.

Attribute Preserving Loss. With the identified attribute bases above that represent important key identifying attributes which should be retained, we introduce our attribute preserving loss to fine-tune the adapter ($\Delta\phi$) to disentangle its editing effects, avoiding the editing of identifying attributes of the avatar. In other words, when users adjust the scale factor (α) to perform editing, we expect the other key attributes to remain unchanged, as if the adapter is not applied for those other attributes. Thus, the attribute preserving loss \mathcal{L}_{AP} can be defined as:

$$\mathcal{L}_{AP}(\Delta\phi) = \mathbb{E}_\alpha \left[\sum_{k=1}^K \|\text{Proj}(\mathbf{f}(\alpha, \Delta\phi, c_{nu}), \mathbf{b}_{a,k}) - \text{Proj}(\mathbf{f}(\emptyset, c_{nu}), \mathbf{b}_{a,k})\|^2 \right], \quad (5)$$

where $\mathbf{f}(\emptyset, c_{nu})$ represents the original latent features without applying the adapter, and various values of α are selected in the range $[-1, 1]$. Intuitively, this loss compares the features after slider adaptation with the features that have not undergone adaptation, comparing them along a few key orthogonal dimensions that represent the key attributes of the avatar which should be retained. Importantly, this loss helps to optimize the adapter parameters ($\Delta\phi$) to disentangle the effects of editing along the concept axis from the other main attributes and dimensions that are not related to the concept axis, encouraging the other attributes to be retained.

Overall, by applying both the sliding loss \mathcal{L}_{CS} (Eq. 3) and the attribute preserving loss \mathcal{L}_{AP} (Eq. 5) to fine-tune the adapter $\Delta\phi$ (see Fig. 2(a)), the model gains the ability to perform precise concept-specific editing via the SDS optimization pipeline in Eq. 1. Thus, when the user manipulates the scale factor α at deployment time, the model can edit the 3D avatar towards a precise point along the concept axis, while maintaining the key identifying features.

4.3. Concept-sensitive 3DGS Primitive Selection

The previous subsections introduced two loss criteria to fine-tune a concept-specific diffusion adapter, enabling precise control of avatar concepts through the SDS optimization pipeline. Here, we further explore a technique to reduce redundant computations, further improving the efficiency of 3D human avatar editing, specifically for avatars in the 3D Gaussian Splatting (3DGS) representation.

3DGS is known for its efficiency in rendering and optimization [17, 21, 26], and has recently been of great interest for generation of 3D objects [6, 33, 38] and 3D humans [21]. Thus, considering its efficiency, we adopt the 3DGS representation for our 3D avatars. The 3DGS representation consists of a set of M Gaussian primitives which we denote as $\{\boldsymbol{\theta}_i\}_{i=1}^M$, where each i -th Gaussian primitive contains a set of parameters $\{\boldsymbol{\mu}_i, \boldsymbol{\Sigma}_i, \sigma_i, \mathbf{h}_i\}$ that determine their location ($\boldsymbol{\mu}_i$), shape ($\boldsymbol{\Sigma}_i$), opacity (σ_i), and color (\mathbf{h}_i). During rendering, the color of each pixel is computed based on all the parameters of all M primitives $\{\boldsymbol{\theta}_i\}_{i=1}^M$ in a differentiable manner, which facilitates the backpropagation of gradients.

However, we find that optimizing the entire 3DGS representation (i.e., all M primitives) yields sub-optimal results for 3D editing. This is because, not all primitives contribute to the final rendering equally [27], some of them are not so important, and so optimizing all primitives incurs high redundancy and harms optimization and editing efficiency. In addition, our concept-specific 3D editing task typically needs to modify only a small subset of primitives that contribute the most towards the target concept. Thus, we select and edit only a subset of primitives, as discussed below.

Concept-Sensitive Primitive Selection. We propose a primitive selection mechanism based on concept-sensitivity to further improve the efficiency of the 3DGS representation in our editing pipeline. Instead of editing all M 3DGS primitives, we only edit the primitives that contribute the most towards our target concept. To achieve this, our mechanism leverages the concept axes identified in Sec. 4.1 to quantify the contribution for each primitive, by computing a *Concept Sensitivity score* that measures how much each primitive is related to the target concept, i.e., how the changes in the primitive parameters affect the precise location along the concept axis. Then, by selecting primitives with a high Concept Sensitivity score and edit only these primitives, we can effectively reduce the redundancy during the editing stage.

Firstly, to compute the sensitivity of Gaussian primitives with respect to the target concept (i.e., the identified concept axis \mathbf{b}_c in the diffusion model’s latent space as discussed in Sec. 4.1), we need to express our 3D avatar in the same latent space. To do this, we first render our 3D avatar – which is represented by a set of primitives $\{\theta_i\}_{i=1}^M$ – to V randomly sampled views, yielding a set of rendered images. These rendered images are then passed into the diffusion model, to extract a set of latent features as $\{\mathbf{z}_{v,x,y}\}_{v \in [1, V], x \in [1, C]}$, where $\mathbf{z}_{v,x} \in \mathbb{R}^D$. These latent features $\mathbf{z}_{v,x}$ belong to the same latent space as $\mathbf{F}_{p,i,x}$ and $\mathbf{F}_{n,i,x}$ in Sec. 4.1.

Next, we calculate the Concept Sensitivity score based on these latent features. Intuitively, the Concept Sensitivity score measures the sensitivity of each primitive towards the target concept, i.e., how much movement there is along the identified concept axis \mathbf{b}_c given a small change in the primitive’s parameters. To compute this, we first compute the projection of the features $\mathbf{z}_{v,x}$ onto the concept bases \mathbf{b}_c as follows: $\bar{C} = \frac{1}{V} \sum_{v=1}^V \text{Proj}(\mathbf{z}_v, \mathbf{b}_c)$. The higher the values in \bar{C} , the more aligned the 3D human avatar is towards the target concept. Hence, if we take a gradient of \bar{C} with respect to the primitive parameters, it will *measure how much movement* there is along the concept axes, given a small change in the primitive, i.e., the sensitivity of the target concept with respect to each primitive’s parameters. Specifically, for each i -th Gaussian primitive θ_i with parameters $\{\mu_i, \Sigma_i, \theta_i, \mathbf{h}_i\}$, we compute its Concept Sensitivity score S_i as:

$$S_i = \sum_{p_i \in \{\mu_i, \Sigma_i, \sigma_i, \mathbf{h}_i\}} \sum_{l=1}^L \left| \frac{\partial \bar{C}_i}{\partial p_i} \right|, \quad (6)$$

which sums the magnitude of the gradients w.r.t. each parameter, where L is the dimensionality of \bar{C} . The higher the Concept Sensitivity score S_i , the more movement there will be along the concept axes given a small change in the i -th Gaussian primitive, which means that primitive is more crucial to editing of the concept. To select the most important primitives to edit, we pre-define a small fractional threshold γ , such that only the top γM primitives, i.e., $\{\theta_i\}_{i=1}^{\gamma M}$, are selected for SDS optimization, instead of all M primitives. Overall, this leads to significantly improved efficiency.

5. Implementation Details

Fine-tuning Details. We use the Depth-RGB dual branch diffusion model [21] based on SD 2 [31], as our diffusion prior. During fine-tuning, we weight the sliding loss and attribute preserving loss equally (coefficient of 0.5 for each), and use LoRA adapter of rank 8. To maintain good avatar quality, we also include a quality preservation loss, which encourages the the output of the slider at value 1 to match the output of the base diffusion model with positive prompts. This loss helps the slider produce images that match the diffusion model, maintaining the generation quality. We set $N_s = 40$, and sample positive, negative and neutral prompts.

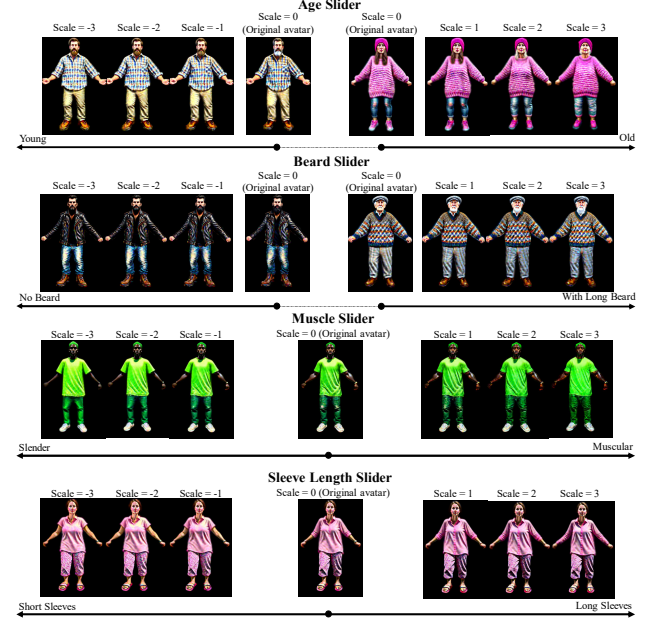


Figure 3. Our editing results using various concept sliders.

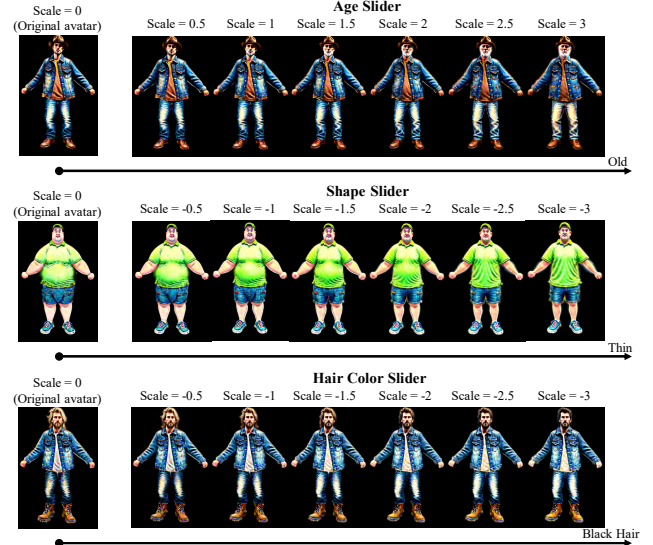


Figure 4. Evaluation of our method’s precise controllability for several concepts. We present the avatars generated across smaller steps (i.e., in steps of 0.5) along the concept sliders.

We set $K = 5$. The adapter is fine-tuned for 1000 steps with batch size 1, using AdamW optimizer (learning rate = $2e - 4$). For each concept-specific adapter, the whole fine-tuning process takes 1 hour and is executed once only.

Avatar Editing Details. We base our 3DGS implementation on the ThreeStudio framework [8] and the optimized renderer from [18]. To obtain source avatars to edit, we generate 3DGS avatars with [21]. Then, following the optimization

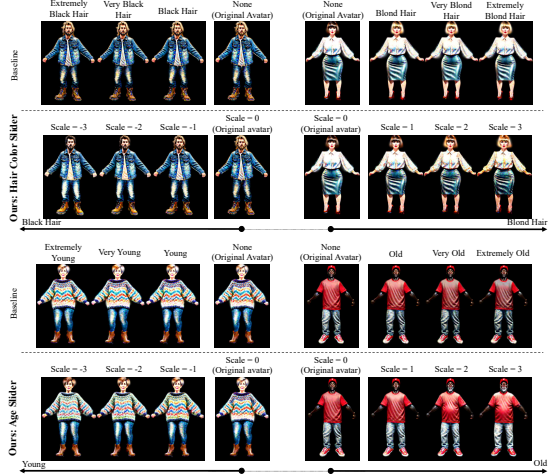


Figure 5. Comparison of our method against existing text-based baseline [21].

settings of [21], we sample the camera distance from range [1.5, 2.0], elevation from range [40, 70], and azimuth from range $[-180, 180]$ with batch size of 4, for each editing update. We set $\gamma = 0.2$. The whole editing process undergoes 1200 updating steps (of SDS optimization). The whole editing process for rendering resolution at 1024 costs 12 minutes on a single NVIDIA 4090 GPU.

6. Experiment Results

In this section, we report and discuss our main results. Please refer to Supp for more results and visualizations.

Qualitative Results. To evaluate our method, we first present editing results across various concepts and avatars in Fig. 3. For each concept, we show results for editing a given avatar by sliding at equally spaced intervals towards the positive (+1, +2, +3) and negative (-1, -2, -3) sides. Results show that our proposed ACS is capable of producing precise changes within the provided avatars effectively, while maintaining their quality and identity. Also note that we only fine-tune our LORA slider within the range [-1,1], yet our ACS shows strong extrapolation ability beyond this range, indicating a well-generalized understanding of the concept.

Precise Editing Results. Next, we further verify our ability for precise control over concepts in Fig. 4, where we adjust the slider in smaller step sizes of 0.5. Our ACS is capable of producing minor changes given small increments in the scale, showing its efficacy at editing concepts precisely.

Comparisons with Baseline. Here, we run baseline comparisons against HumanGaussian [21] which is a widely-used text-driven generation method for producing 3DGS avatars that adhere to text inputs. As a baseline, we adopt their method while altering the text prompts to perform text-based editing, where we modify the text prompts by adding concept-related words (e.g., young, old) and adding adverbs to express degrees of expression, e.g., ‘very’, ‘ex-

Table 2. Efficiency comparisons of our method.

Setting	Time Taken to Converge
NeRF	91 min
3DGS	42 min
Ours	12 min

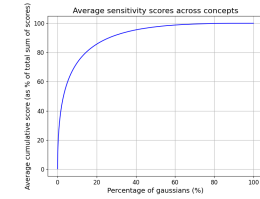


Figure 6. Plot showing the average percentage of Gaussian primitives required to account for a given percentage of the total summed sensitivity scores.

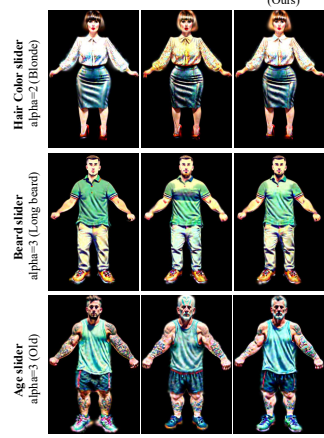


Figure 7. Impact of Attribute Preserving Loss.

tremely’. For fair comparison, source 3DGS avatars for both our method and the baseline are generated using the pipeline of [21]. Our comparison against the baseline is presented in Fig. 5. Crucially, unlike the text-driven baseline, our method offers *precise controllability*, enabling users to select a slider factor to edit the avatar concept to a desired degree. Our edited outcomes also tend to *better align with the provided descriptions*. Please refer to Supp for more comparisons.

User Study. We conduct a user study to show the superiority of our ACS for manipulating the degree of concepts. We invited 30 individuals from the general public to compare our method with the baseline [21]. Each participant was shown 16 sets of edited avatars, with each set containing results from both methods edited to various degrees of a concept. Participants answered three questions regarding editing relevance and quality: (1) Which image shows more relevant results to the editing target? (2) Which image better shows the concept changing from source to target? (3) Which image shows better editing quality? As shown in Tab. 1, users significantly favour our ACS over the baseline.

Table 1. Results of user study.

Setting	User Preference Rate (%)		
	Q1	Q2	Q3
Baseline [21]	15.62	16.67	26.04
Ours	84.38	83.33	73.96

7. More Experiments and Ablation Studies

Impact of Attribute Preserving Loss. In Sec. 4.2, we proposed the Attribute Preserving Loss \mathcal{L}_{AP} to better retain identity information during editing. We visualize the effect of \mathcal{L}_{AP} in Fig. 7, where we observe that it helps to improve the retaining of identity information (e.g., clothing color, hair) during the editing process.

Analysis of Concept-Sensitive Primitive Selection. In our ACS, we further introduce the concept-sensitive selection mechanism to edit only a small fraction of primitives based

on the Concept Sensitivity score. To find out how many primitives are sensitive to the concept on average, we computed the Concept Sensitivity scores of primitives across 5 concepts, where 10 avatars were used for each concept. We summed up the Concept Sensitivity scores (which are non-negative) for each avatar and concept, and plotted the average percentage of primitives required to get a certain percentage of the summed sensitivity scores in Fig. 6. We observe that, on average, across concepts and avatars, about 20% of the primitives account for 85% of the summed Concept Sensitivity scores, which means they receive 85% of the total gradients. Therefore, we set the fractional threshold γ to 0.2 to focus on editing these “concept-sensitive” primitives, improving efficiency while maintaining editing quality. Moreover, Tab. 2 compares the editing speed of our method against a NeRF-based representation [39] and 3DGS baseline [21], using the same diffusion prior. Results show that our ACS is more efficient than the baselines.

8. Conclusion

In this work, we introduce our novel ACS for 3D avatar editing, enabling users to edit their 3D avatar precisely towards the desired degree of expression of a given concept. Our ACS includes a Concept Sliding Loss based on LDA and Attribute Preserving Loss based on PCA. We also introduce a concept-sensitivity selection mechanism for improved editing efficiency. Results show that ACS enables controllable and concept-specific avatar editing, while maintaining the quality of the avatars.

References

- [1] Md Shahinur Alam, Jason Lamberton, Jianye Wang, Carly Leannah, Sarah Miller, Joseph Palagano, Myles de Bastion, Heather L. Smith, Melissa Malzkuhn, and Lorna C. Quandt. Asl champ!: A virtual reality game with deep-learning driven sign recognition, 2023. [1](#)
- [2] Shivangi Aneja, Justus Thies, Angela Dai, and Matthias Nießner. Clipface: Text-guided editing of textured 3d morphable models. In ACM SIGGRAPH 2023 Conference Proceedings, SIGGRAPH 2023, Los Angeles, CA, USA, August 6-10, 2023, pages 70:1–70:11. ACM, 2023. [1](#), [2](#)
- [3] Tim Brooks, Aleksander Holynski, and Alexei A. Efros. Instructpix2pix: Learning to follow image editing instructions. In IEEE/CVF Conference on Computer Vision and Pattern Recognition, CVPR 2023, Vancouver, BC, Canada, June 17-24, 2023, pages 18392–18402. IEEE, 2023. [1](#)
- [4] Yukang Cao, Yan-Pei Cao, Kai Han, Ying Shan, and Kwan-Yee K. Wong. Dreamavatar: Text-and-shape guided 3d human avatar generation via diffusion models. CoRR, abs/2304.00916, 2023. [1](#), [2](#), [3](#)
- [5] Yiwen Chen, Zilong Chen, Chi Zhang, Feng Wang, Xiaofeng Yang, Yikai Wang, Zhongang Cai, Lei Yang, Huaping Liu, and Guosheng Lin. Gaussianeditor: Swift and controllable 3d editing with gaussian splatting. CoRR, abs/2311.14521, 2023. [2](#)
- [6] Zilong Chen, Feng Wang, Yikai Wang, and Huaping Liu. Text-to-3d using gaussian splatting. In Proceedings of the IEEE/CVF conference on computer vision and pattern recognition, pages 21401–21412, 2024. [6](#)
- [7] Rohit Gandikota, Joanna Materzyńska, Tingrui Zhou, Antonio Torralba, and David Bau. Concept sliders: Lora adaptors for precise control in diffusion models. In European Conference on Computer Vision, pages 172–188. Springer, 2024. [3](#)
- [8] Yuan-Chen Guo, Ying-Tian Liu, Ruizhi Shao, Christian Laforte, Vikram Voleti, Guan Luo, Chia-Hao Chen, Zi-Xin Zou, Chen Wang, Yan-Pei Cao, and Song-Hai Zhang. threestudio: A unified framework for 3d content generation. <https://github.com/threestudio-project/threestudio>, 2023. [7](#)
- [9] Xiao Han, Yukang Cao, Kai Han, Xiatian Zhu, Jiankang Deng, Yi-Zhe Song, Tao Xiang, and Kwan-Yee K. Wong. Headsculpt: Crafting 3d head avatars with text. CoRR, abs/2306.03038, 2023. [1](#), [2](#), [3](#)
- [10] Ayaan Haque, Matthew Tancik, Alexei A. Efros, Aleksander Holynski, and Angjoo Kanazawa. Instructnerf2nerf: Editing 3d scenes with instructions. CoRR, abs/2303.12789, 2023. [2](#)
- [11] Trevor Hastie, Robert Tibshirani, Jerome H Friedman, and Jerome H Friedman. *The elements of statistical learning: data mining, inference, and prediction*. Springer, 2009. [4](#)
- [12] Fangzhou Hong, Mingyuan Zhang, Liang Pan, Zhongang Cai, Lei Yang, and Ziwei Liu. Avatarclip: zero-shot text-driven generation and animation of 3d avatars. ACM Trans. Graph., 41(4):161:1–161:19, 2022. [1](#), [2](#)
- [13] Edward J. Hu, Yelong Shen, Phillip Wallis, Zeyuan Allen-Zhu, Yuanzhi Li, Shean Wang, Lu Wang, and Weizhu Chen. Lora: Low-rank adaptation of large language models. In The Tenth International Conference on Learning Representations, ICLR 2022, Virtual Event, April 25-29, 2022. OpenReview.net, 2022. [3](#)
- [14] Yukun Huang, Jianan Wang, Ailing Zeng, He Cao, Xianbiao Qi, Yukai Shi, Zheng-Jun Zha, and Lei Zhang. Dreamwaltz: Make a scene with complex 3d animatable avatars. CoRR, abs/2305.12529, 2023. [1](#), [2](#)
- [15] Ruixiang Jiang, Can Wang, Jingbo Zhang, Menglei Chai, Mingming He, Dongdong Chen, and Jing Liao. Avatarcraft: Transforming text into neural human avatars with parameterized shape and pose control. CoRR, abs/2303.17606, 2023. [1](#), [2](#), [3](#)

[16] Zeyinzi Jiang, Chaojie Mao, Yulin Pan, Zhen Han, and Jingfeng Zhang. Scedit: Efficient and controllable image diffusion generation via skip connection editing. In *Proceedings of the IEEE/CVF conference on computer vision and pattern Recognition*, pages 8995–9004, 2024. 3

[17] Kai Katsumata, Duc Minh Vo, and Hideki Nakayama. An efficient 3d gaussian representation for monocular/multi-view dynamic scenes, 2023. 6

[18] Bernhard Kerbl, Georgios Kopanas, Thomas Leimkühler, and George Drettakis. 3d gaussian splatting for real-time radiance field rendering. *ACM Trans. Graph.*, 42(4):139:1–139:14, 2023. 3, 7

[19] Nikos Kolotouros, Thieno Alldieck, Andrei Zanfir, Eduard Gabriel Bazavan, Mihai Fieraru, and Cristian Sminchisescu. Dreamhuman: Animatable 3d avatars from text. *CoRR*, abs/2306.09329, 2023. 1, 2

[20] Chen-Hsuan Lin, Jun Gao, Luming Tang, Towaki Takikawa, Xiaohui Zeng, Xun Huang, Karsten Kreis, Sanja Fidler, Ming-Yu Liu, and Tsung-Yi Lin. Magic3d: High-resolution text-to-3d content creation. In *IEEE/CVF Conference on Computer Vision and Pattern Recognition, CVPR 2023, Vancouver, BC, Canada, June 17-24, 2023*, pages 300–309. IEEE, 2023. 1, 3

[21] Xian Liu, Xiaohang Zhan, Jiaxiang Tang, Ying Shan, Gang Zeng, Dahua Lin, Xihui Liu, and Ziwei Liu. Humaugaussian: Text-driven 3d human generation with gaussian splatting. *CoRR*, abs/2311.17061, 2023. 1, 2, 6, 7, 8, 9

[22] Timo Lüdecke and Alexander S. Ecker. Image segmentation using text and image prompts. In *IEEE/CVF Conference on Computer Vision and Pattern Recognition, CVPR 2022, New Orleans, LA, USA, June 18-24, 2022*, pages 7076–7086. IEEE, 2022. 2

[23] Geoffrey J McLachlan. *Discriminant analysis and statistical pattern recognition*. John Wiley & Sons, 2005. 4

[24] Mohit Mendiratta, Xingang Pan, Mohamed Elgharib, Kartik Teotia, Mallikarjun B. R., Ayush Tewari, Vladislav Golyanik, Adam Kortylewski, and Christian Theobalt. Avatarstudio: Text-driven editing of 3d dynamic human head avatars. *ACM Trans. Graph.*, 42(6):226:1–226:18, 2023. 1, 2, 3

[25] Ben Mildenhall, Pratul P. Srinivasan, Matthew Tancik, Jonathan T. Barron, Ravi Ramamoorthi, and Ren Ng. Nerf: Representing scenes as neural radiance fields for view synthesis. In *Computer Vision - ECCV 2020 - 16th European Conference, Glasgow, UK, August 23-28, 2020, Proceedings, Part I*, pages 405–421. Springer, 2020. 3

[26] Arthur Moreau, Jifei Song, Helisa Dhamo, Richard Shaw, Yiren Zhou, and Eduardo Pérez-Pellitero. Human gaussian splatting: Real-time rendering of animatable avatars. In *Proceedings of the IEEE/CVF conference on computer vision and pattern recognition*, pages 788–798, 2024. 6

[27] Simon Niedermayr, Josef Stumpfegger, and Rüdiger Westermann. Compressed 3d gaussian splatting for accelerated novel view synthesis. In *Proceedings of the IEEE/CVF Conference on Computer Vision and Pattern Recognition*, pages 10349–10358, 2024. 6

[28] Ben Poole, Ajay Jain, Jonathan T. Barron, and Ben Mildenhall. Dreamfusion: Text-to-3d using 2d diffusion. In *The Eleventh International Conference on Learning Representations, ICLR 2023, Kigali, Rwanda, May 1-5, 2023*. OpenReview.net, 2023. 1, 2, 3

[29] Alec Radford, Jong Wook Kim, Chris Hallacy, Aditya Ramesh, Gabriel Goh, Sandhini Agarwal, Girish Sastry, Amanda Askell, Pamela Mishkin, Jack Clark, Gretchen Krueger, and Ilya Sutskever. Learning transferable visual models from natural language supervision. In *Proceedings of the 38th International Conference on Machine Learning, ICML 2021, 18-24 July 2021, Virtual Event*, pages 8748–8763. PMLR, 2021. 2

[30] Robin Rombach, Andreas Blattmann, Dominik Lorenz, Patrick Esser, and Björn Ommer. High-resolution image synthesis with latent diffusion models. In *IEEE/CVF Conference on Computer Vision and Pattern Recognition, CVPR 2022, New Orleans, LA, USA, June 18-24, 2022*, pages 10674–10685. IEEE, 2022. 2, 3

[31] Robin Rombach, Andreas Blattmann, Dominik Lorenz, Patrick Esser, and Björn Ommer. High-resolution image synthesis with latent diffusion models. In *Proceedings of the IEEE/CVF Conference on Computer Vision and Pattern Recognition (CVPR)*, pages 10684–10695, 2022. 7

[32] Basavaraj Sunagad, Heming Zhu, Mohit Mendiratta, Adam Kortylewski, Christian Theobalt, and Marc Habermann. Tedra: Text-based editing of dynamic and photoreal actors. *arXiv preprint arXiv:2408.15995*, 2024. 2

[33] Jiaxiang Tang, Jiawei Ren, Hang Zhou, Ziwei Liu, and Gang Zeng. Dreamgaussian: Generative gaussian splatting for efficient 3d content creation. *CoRR*, abs/2309.16653, 2023. 6

[34] Kartik Teotia, Mallikarjun B. R., Xingang Pan, Hyeongwoo Kim, Pablo Garrido, Mohamed Elgharib, and Christian Theobalt. Hq3davatar: High quality controllable 3d head avatar. *CoRR*, abs/2303.14471, 2023. 2

[35] Qian Wan and Zhicong Lu. Investigating vtubing as a

reconstruction of streamer self-presentation: Identity, performance, and gender, 2023. 1

[36] Zhengyi Wang, Cheng Lu, Yikai Wang, Fan Bao, Chongxuan Li, Hang Su, and Jun Zhu. Prolificdreamer: High-fidelity and diverse text-to-3d generation with variational score distillation. *CoRR*, abs/2305.16213, 2023. 1

[37] Yichao Yan, Zanwei Zhou, Zi Wang, Jingnan Gao, and Xiaokang Yang. Dialoguenerf: Towards realistic avatar face-to-face conversation video generation, 2023. 1

[38] Taoran Yi, Jiemin Fang, Junjie Wang, Guanjun Wu, Lingxi Xie, Xiaopeng Zhang, Wenyu Liu, Qi Tian, and Xinggang Wang. Gaussiandreamer: Fast generation from text to 3d gaussians by bridging 2d and 3d diffusion models. In *Proceedings of the IEEE/CVF Conference on Computer Vision and Pattern Recognition*, pages 6796–6807, 2024. 6

[39] Huichao Zhang, Bowen Chen, Hao Yang, Liao Qu, Xu Wang, Li Chen, Chao Long, Feida Zhu, Kang Du, and Min Zheng. Avatarverse: High-quality & stable 3d avatar creation from text and pose. *CoRR*, abs/2308.03610, 2023. 1, 2, 3, 9

[40] Hao Zhang, Yao Feng, Peter Kulis, Yandong Wen, Justus Thies, and Michael J. Black. Text-guided generation and editing of compositional 3d avatars. *CoRR*, abs/2309.07125, 2023. 1, 2, 3

[41] Jianfeng Zhang, Xuanmeng Zhang, Huichao Zhang, Jun Hao Liew, Chenxu Zhang, Yi Yang, and Jiashi Feng. Avatarstudio: High-fidelity and animatable 3d avatar creation from text. *CoRR*, abs/2311.17917, 2023. 2

[42] Lvmin Zhang and Maneesh Agrawala. Adding conditional control to text-to-image diffusion models. *CoRR*, abs/2302.05543, 2023. 2

[43] Lvmin Zhang, Anyi Rao, and Maneesh Agrawala. Adding conditional control to text-to-image diffusion models. In *Proceedings of the IEEE/CVF international conference on computer vision*, pages 3836–3847, 2023. 3

[44] Guangcong Zheng, Xianpan Zhou, Xuewei Li, Zhonggang Qi, Ying Shan, and Xi Li. Layoutdiffusion: Controllable diffusion model for layout-to-image generation. In *Proceedings of the IEEE/CVF Conference on Computer Vision and Pattern Recognition*, pages 22490–22499, 2023. 3

[45] Jingyu Zhuang, Chen Wang, Liang Lin, Lingjie Liu, and Guanbin Li. Dreameditor: Text-driven 3d scene editing with neural fields. In *SIGGRAPH Asia 2023 Conference Papers, SA 2023, Sydney, NSW, Australia, December 12-15, 2023*, pages 26:1–26:10. ACM, 2023. 2